

Low-level accretion in neutron-star X-ray binaries

R. Wijnands^{1*}, N. Degenaar², M. Armas Padilla^{3,4†}, D. Altamirano^{5‡}, Y. Cavecchi¹, M. Linares^{3,4}, A. Bahramian⁶, C. O. Heinke^{6,7§}

¹*Astronomical Institute Anton Pannekoek, University of Amsterdam, Postbus 94249, 1090 GE Amsterdam, The Netherlands*

²*Institute of Astronomy, University of Cambridge, Madingley Road, Cambridge, CB3 0HA, UK*

³*Instituto de Astrofísica de Canarias, c/ Vía Láctea s/n, E-38205 La Laguna, Tenerife, Spain*

⁴*Departamento de Astrofísica, Universidad de la Laguna, La Laguna, E-38205, S/C de Tenerife, Spain*

⁵*Physics & Astronomy, University of Southampton, Southampton, Hampshire SO17 1BJ, UK*

⁶*Department of Physics, University of Alberta, CCIS 4-183, Edmonton, AB T6G 2E1, Canada*

⁷*Max-Planck-Institut für Radioastronomie, Auf dem Hügel 69, D-53121 Bonn, Germany*

28 October 2018

ABSTRACT

We search the literature for reports on the spectral properties of neutron-star low-mass X-ray binaries when they have accretion luminosities between 10^{34} and 10^{36} ergs s^{-1} , corresponding to roughly 0.01% - 1% of the Eddington accretion rate for a neutron star. We found that in this luminosity range the photon index (obtained from fitting a simple absorbed power-law in the 0.5–10 keV range) increases with decreasing 0.5–10 keV X-ray luminosity (i.e., the spectrum softens). Such behaviour has been reported before for individual sources, but here we demonstrate that very likely most (if not all) neutron-star systems behave in a similar manner and possibly even follow a universal relation. When comparing the neutron-star systems with black-hole systems, it is clear that most black-hole binaries have significantly harder spectra at luminosities of $10^{34} - 10^{35}$ erg s^{-1} . Despite a limited number of data points, there are indications that these spectral differences also extend to the $10^{35} - 10^{36}$ erg s^{-1} range, but above a luminosity of 10^{35} erg s^{-1} the separation between neutron-star and black-hole systems is not as clear as below. In addition, the black-hole spectra only become softer below luminosities of 10^{34} erg s^{-1} compared to 10^{36} erg s^{-1} for the neutron-star systems. This observed difference between the neutron-star binaries and black-hole ones suggests that the spectral properties (between 0.5–10 keV) at $10^{34} - 10^{35}$ erg s^{-1} can be used to tentatively determine the nature of the accretor in unclassified X-ray binaries. More observations in this luminosity range are needed to determine how robust this diagnostic tool is and whether or not there are (many) systems that do not follow the general trend. We discuss our results in the context of properties of the accretion flow at low luminosities and we suggest that the observed spectral differences likely arise from the neutron-star surface becoming dominantly visible in the X-ray spectra. We also suggest that both the thermal component *and* the non-thermal component might be caused by low-level accretion onto the neutron-star surface for luminosities below a few times 10^{34} erg s^{-1} .

Key words: X-rays: binaries - binaries: close - accretion, accretion disc

1 INTRODUCTION

In low-mass X-ray binaries (LMXBs), a compact object (a black hole or a neutron star) is accreting matter from a com-

panion star which typically has a mass (often significantly) lower than that of the accretor. The matter is transferred because the donor fills its Roche lobe. Most LMXBs are so-called X-ray transients: they exhibit sporadic outbursts during which the X-ray luminosity (0.5–10 keV; from here on we use this energy range when quoting luminosities, unless otherwise mentioned) increases up to a few times $10^{38} - 10^{39}$ erg s^{-1} , although many systems do not become this bright and some only reach very faint luminosities of $10^{34} - 10^{36}$

* r.a.d.wijnands@uva.nl

† CEI Canarias: Campus Atlántico tricontinental

‡ University Research Fellow

§ Alexander von Humboldt Fellow

erg s⁻¹ (the so-called very-faint X-ray transients; see, e.g., the discussion in Wijnands et al. 2006)¹. However, most of the time these X-ray transients are in their quiescent state during which no or hardly any accretion occurs and consequently their X-ray luminosities are extremely low (typically 10³⁰ – 10³³ erg s⁻¹).

Ever since LMXBs were first discovered in the late 1960's, they have been studied intensively using all available X-ray instruments. Therefore, their observational properties are well characterized, at least at X-ray luminosities above ~ 10³⁶ erg s⁻¹. This is mainly due to the limited sensitivity of most X-ray instruments in orbit in combination with the limited amount of observing time which can be obtained with high sensitivity instruments when those X-ray binaries are at very faint luminosities. Consequently, despite the increasing amount of data over the last decade, the X-ray behaviour of LMXBs at luminosities of 10³⁴–³⁶ erg s⁻¹ is not yet understood. We note that for the purpose of this paper we define systems which are below an X-ray luminosity of 10³⁴ erg s⁻¹ as quiescent X-ray transients.

The spectral behaviour of LMXBs above 10³⁶ erg s⁻¹ is relatively well understood (see, e.g., discussions in Remillard & McClintock 2006; Lin et al. 2007). At lower accretion luminosities, the phenomenological behaviour is significantly less clear. Over the last few years, a growing number of very-faint X-ray binaries have been spectrally studied and the general conclusion is that the sources can often be satisfactorily described with a simple power-law model, although more complex models cannot be excluded because of the limitations imposed by the data quality. However, irrespectively of what model is fitted to the spectra, they become softer with decreasing luminosity. This appears to be true for both black-hole and neutron-star systems (see, e.g., Armas Padilla et al. 2011, 2013a; Plotkin et al. 2013; Reynolds et al. 2014; Yang et al. 2015, and references therein).

For black-hole systems, this softening is typically explained in the context of a radiative inefficient accretion flow (e.g., see the discussion in Plotkin et al. 2013; Reynolds et al. 2014). Similar explanations have been proposed for the neutron-star systems (see, e.g., Armas Padilla et al. 2011, 2013b). However, when high quality data are obtained from the neutron-star systems, the spectrum cannot easily be described with a simple power-law model anymore, but requires an additional soft component (e.g., Degenaar et al. 2013; Armas Padilla et al. 2013b,c). Likely this soft emission originates from the surface of the neutron star, e.g., due to low-level accretion onto the surface which might produce such type of spectra (e.g., Zampieri et al. 1995; Deufel et al. 2001). This additional spectral component complicates the interpretation of the softening. It is currently unclear if the softening seen in neutron star systems is due to this soft thermal component becoming dominant with no change in the power-law component, or if also the power-law component

evolves with decreasing luminosity (see the discussions in Armas Padilla et al. 2013b,c).

To obtain more insight into these topics, we performed a detailed literature study about what is currently known about the spectra of neutron-star X-ray binaries when they have accretion luminosities between 10³⁴ and 10³⁶ erg s⁻¹. We will also compare those systems with the black-hole transients at similar luminosities. We do not use the symbiotic neutron-star LMXBs (see Lü et al. 2012, for a compilation of known systems) in our analysis since in those systems the neutron star accretes from a stellar wind and not from a disk. In addition, most symbiotic systems harbour a neutron star with a strong magnetic field (typically > 10¹² Gauss). Such a strong field will significantly alter the emerging spectra and therefore those systems cannot be directly compared with the systems which have a weak or absent magnetic field (< 10¹⁰ Gauss). For the same reason we also do not include the high-magnetic field (also typically > 10¹² Gauss) neutron-star systems in which the mass transfer does occur through Roche-lobe overflow and in which an accretion disk is present (e.g., 4U 1626–67, 4U 1822–37, GRO J1744–28).

2 DATA SELECTION AND RESULTS

We searched the literature for publications that describe spectral results on neutron-star LMXBs (both transients as well as persistent systems) which are not in quiescence (thus above 10³⁴ erg s⁻¹; see section 2.3 for the justification of this lower luminosity boundary), but below a X-ray luminosity of a few times 10³⁶ erg s⁻¹. Since it is unclear if a dynamically important neutron-star magnetic field could alter the observed X-ray spectra, we initially only use the non-pulsating systems². In section 2.2 we compare the non-pulsating systems with the accreting millisecond X-ray pulsars to investigate if indeed magnetic field effects could be observed in the X-ray spectra in neutron-star LMXBs.

We limited ourselves to those publications which reported on observations that covered the 0.5–10 keV energy range, so that accurate measurements could be obtained for the spectral shape below ~2 keV. In addition, those systems that have a column density of $N_{\text{H}} > 5 \times 10^{22}$ cm⁻² were excluded from our source selection because their spectra below 2 keV cannot be accurately modelled. Extrapolation from the 2–10 keV fit results down to 0.5 keV can result in significant systematic errors. This criterion excludes most sources close to the Galactic centre (e.g., those reported on by Wijnands et al. 2002; Muno et al. 2003, 2005; Sakano et al. 2005; Porquet et al. 2005; Del Santo et al. 2007; Degenaar & Wijnands 2009, 2010, 2013; Degenaar et al. 2011, 2012b). In section 3.3 we will briefly discuss those sources and how including them in our source sample would affect our conclusions.

In most publications the spectral results were reported

¹ Although Wijnands et al. (2006) used the 2–10 keV energy range to classify the sources, we use in this paper the 0.5–10 keV energy range in order to study the spectral evolution also below 2 keV.

² Aql X-1 has shown a very brief episode during which it exhibited X-ray pulsations (Casella et al. 2008), but the vast majority of its time it does not exhibit such oscillations and its general X-ray spectral and timing behaviour resembles other non-pulsating LMXBs. Therefore, we included this source in our non-pulsating sample.

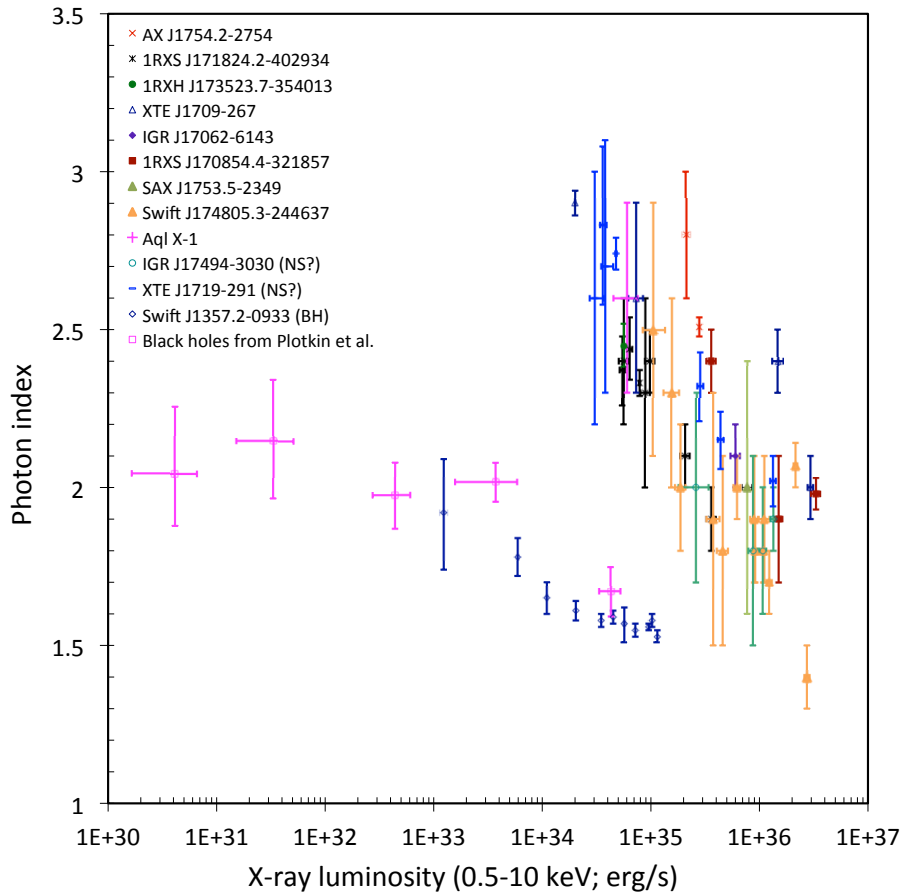


Figure 1. The photon index versus the 0.5–10 keV X-ray luminosity for the neutron-star X-ray binaries used in this paper (Tab. 1) as well as for the black-hole system Swift J1357.2–0933 (Armas Padilla et al. 2013a) and the average of the black-hole points from Plotkin et al. (2013). (A colour version of this figure is available in the online version of this paper.)

when using a simple absorbed power-law model, but often also a two-component model was used: a thermal component at low energies and a power-law component at high energies (e.g., Jonker et al. 2004b; Fridriksson et al. 2010; Degenaar et al. 2013; Armas Padilla et al. 2013b; Campana et al. 2008, 2014). Sadly, no uniform model was used (e.g., for the thermal component either a black-body model or a neutron-star atmosphere model was used; e.g., Jonker et al. 2004b; Armas Padilla et al. 2013b,c) making global comparisons between sources difficult. Since for most sources the results of a single power-law model were reported (which typically resulted in acceptable fits), we will focus on that model in this paper. When a two-component model was used and no results were reported on a single power-law model (e.g., in Fridriksson et al. 2010, 2011; Campana et al. 2008, 2014), we did not include those points in our selection. Photon indices (Γ) obtained from fitting a two-component model are typically very different from those obtained with a single power-law model. This is clear from the papers where

both types of fits are reported (e.g., Armas Padilla et al. 2013b).

In some publications where the sources were fitted with a single power-law model, the errors on the obtained photon indices were so large that no significant conclusions can be obtained from those data points. Therefore, we do not use those data points for which the photon indices had an error larger than 0.5. This excludes the results in several publications such as those reported for SAX J1750.8–2900 (Lowell et al. 2012; Wijnands & Degenaar 2013; Allen et al. 2015), SAX J1828.5–1037 (Degenaar & Wijnands 2008; Campana 2009), or Swift J1749.4–2807 (Wijnands et al. 2009; Campana 2009). In addition, this excludes some of the data points for some of the sources we do use in this paper (e.g., some data points of Swift J174805.3–244637; Bahramian et al. 2014).

Degenaar et al. (2012d) reported on monitoring observations using *Swift* of two newly discovered neutron-star X-ray transients: Swift J185003.2–005627 and Swift J1922.7–1716. Also in that paper the reported results were based

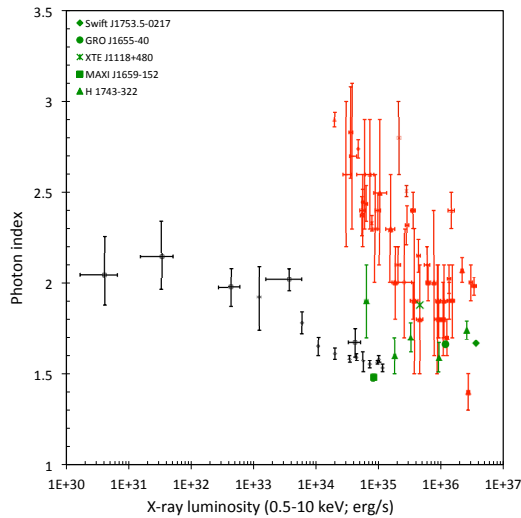


Figure 2. Adapted from Figure 1. The red points are the neutron-star systems and the black points the black-hole transients. In addition, the figure now includes several additional black-hole X-ray transients with luminosities in the range 10^{34} to 10^{36} erg s^{-1} (the green points). (A colour version of this figure is available in the online version of this paper.)

mostly on a two component model to fit the source spectra (see also Falanga et al. 2006, for Swift J1922.7–1716) but they also listed the results obtained using a single power-law model. However, those results were obtained from a spectral fit to the combined data set including a range of X-ray luminosities so that any possible evolution of the X-ray spectral shape with luminosity is averaged out. Therefore, we also do not include these results in our analysis. We note that for Swift J18500.3–005627, Degenaar et al. (2012d) found that (when studying the X-ray colours) the source softened when the X-ray luminosity decreases. This would be consistent with the general trend for neutron-star X-ray binaries we report on below.

Our resulting sample of neutron-star X-ray binaries is listed in Table 1. We have included all sources in our sample for which we found results in the published literature. However, it is conceivable that we did not find all the relevant publications and that therefore some sources could have been missed. However, we feel that that would only be a very low number of sources and therefore the sources used in our paper should serve as a representative sample of the whole population. Among our eleven sources, three are persistently accreting at 10^{34} – 10^{35} erg s^{-1} and eight are X-ray transients (see Tab. 1). Nine sources are confirmed neutron-star binaries since type-I X-ray bursts have been seen, and two are strong neutron-star candidates (see section 4.4). In Figure 1 we plot the photon indices of those eleven sources versus their 0.5–10 keV X-ray luminosities. Although there is a large scatter in the points, the neutron-star systems follow a clear trend: on average the photon index is between 1.5 and 2 for X-ray luminosities of $\sim 10^{36}$ erg s^{-1} , but it increases

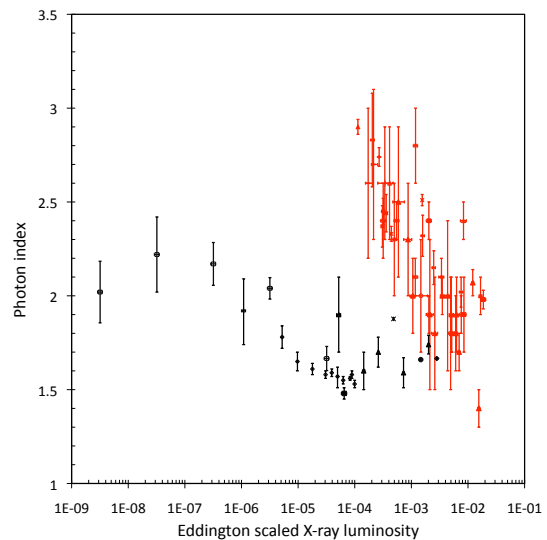


Figure 3. Adapted from Figure 2 but scaled to the Eddington X-ray luminosity (the black points are the black-hole systems; the red points the neutron-star ones; a colour version of this figure is available in the online version of this paper).

to 2–3 (i.e., the overall X-ray spectrum becomes softer) when the X-ray luminosity decreases. This was observed already from some individual sources that showed a large dynamic range in luminosity (see, e.g., Armas Padilla et al. 2011; Bahramian et al. 2014; Linares et al. 2014) but from Figure 1 it can now be seen that all neutron-star systems in our sample follow in general a similar behaviour.

We performed several correlation tests to determine if indeed the photon index is correlated with the luminosity. A Pearson test, Spearman test, and a Kendall test resulted in correlation indices of -0.81 , -0.77 , and -0.60 , respectively, corresponding to a probability of 1.78×10^{-11} , 4.83×10^{-10} , and 6.84×10^{-9} , respectively, that both parameters are uncorrelated. Therefore, we consider these results a support for our conclusions that the photon index is indeed anti-correlated with the luminosity. We fitted a power law of the shape $\Gamma = a \log L_X + b$ to the data and we obtained the following parameters: $a = -0.42 \pm 0.03$ and $b = 17.3 \pm 1.1$ (90% confidence levels). To quantify the scatter around this correlation we calculated the root-mean-square of deviations from the correlation and found a value of 0.28.

2.1 Comparison with black-hole X-ray binaries

To compare our result obtained for the neutron-star LMXBs with black-hole systems, we used the data reported by Plotkin et al. (2013) who discussed the behaviour of black-hole X-ray transients as they decayed down to quiescence. We applied the same selection criteria as we used for our neutron-star sample to the individual black-hole points reported by Plotkin et al. (2013, their Table 3 and 5). We averaged the photon indices and calculated the corresponding errors. We averaged the luminosities and as errors we

used the standard deviation on those luminosity points. In addition, we used the points of Swift J1357.2-0933 from Armas Padilla et al. (2013a, we used the averaged points used to create their Figure 1, right panels; the values of those points are not listed in this reference, so we list them in Table 2). Clearly, the black-hole points are significantly offset from the neutron-star points in Figure 1.

We searched the literature for more black-hole transients with luminosities between 10^{35} and 10^{37} erg s $^{-1}$ but not many could be found. The ones we found are listed in Table 2 and shown in Figure. 2. Even though in the luminosity range of $10^{35} - 10^{36}$ erg s $^{-1}$ the black-hole systems appear to be on average harder than the neutron-star binaries, there is a significant overlap of the data points (especially above $\sim 5 \times 10^{35}$ erg s $^{-1}$). We only have a few black-hole systems in this luminosity range making final conclusions on the average hardness of those systems in this range difficult. In any case, it seems that above 10^{35} erg s $^{-1}$ the neutron-star binaries are not as clearly separated from the black-hole transients as at luminosities below 10^{35} erg s $^{-1}$ (even more so when also including the accreting millisecond X-ray pulsars, which are discussed in section 2.2).

We used a 2D Kolmogorov-Smirnov (KS) test (see Fasano & Franceschini 1987) on the neutron-star and black-hole data points to quantify the probability that the two samples are drawn from two different distributions, therefore confirming that they behave differently. However, the KS test does not account directly for the errors in the measurements of photon index and luminosity. In order to account for such errors we generated 10^5 synthetic samples randomly shifting each source around the reported values. We assumed a Gaussian distribution with standard deviations conservatively given by the reported errors on the measurements. First, we compared the full data sets of neutron stars and black hole; the black hole sample included the (not averaged) values of Plotkin et al. (2013), as well as the other black hole data (see Fig. 4 and section 2.1.1). Assuming a null hypothesis that the two distributions are the same, we obtained a 90 % confidence interval for the probability of $2.4 \times 10^{-14} - 3.3 \times 10^{-11}$. This result strongly supports our idea that the two data sets are drawn from different distributions. However, many black-hole data points have luminosities below 10^{34} erg s $^{-1}$; that may influence the results of the test, since no neutron-star systems were include below that threshold. To avoid biasing the results, we repeated the test keeping only the black-hole data points with luminosities above 10^{34} erg/s. In this case the 90 % confidence interval for the probability that the two sets come from the same distribution is higher, but still it is very low, being only $2.8 \times 10^{-7} - 2.7 \times 10^{-5}$. Despite the low number of data points, we conclude that the 2D KS test supports our idea that the two kind of systems behave markedly differently.

Plotkin et al. (2013) used the luminosities scaled to the Eddington luminosity when discussing the black-hole systems. For quiescent X-ray transients there are physical reasons for doing this (see, e.g., Menou et al. 1999) but it is unclear if those reasons also apply when the sources are not in quiescence. However, for completeness, in Figure 3 we replotted our data set with the X-ray luminosity in Eddington units. We used the Eddington scaled values from Plotkin et al. (2013) as presented in their Figure 4b. We converted the points of Swift J1357.2-09333

(from Armas Padilla et al. 2013a) using a black-hole mass of $9 M_{\odot}$, and we used the same black-hole masses used by Plotkin et al. (2013) for the other black holes (except for Swift J1753.5-0127 for which we assumed $10 M_{\odot}$ since this source was not included in the study of Plotkin et al. 2013). We converted the neutron-star values using a neutron-star mass of $1.4 M_{\odot}$ (resulting in an Eddington luminosity of 1.8×10^{38} erg s $^{-1}$). It is clear that when using Eddington scaled luminosities, the difference between the neutron-star systems and the black-hole systems becomes even more pronounced. We note that when using the Eddington scaled luminosities, an additional uncertainty is introduced because of the uncertainties in the mass of the accretors. Most black-hole masses are poorly constrained and also the neutron-star masses could display a range (e.g., from 1.2 up to $2 M_{\odot}$). Therefore, from here on, we only show the X-ray luminosities in our figures and not the Eddington scaled one since this allows for direct comparison of different source types without assuming anything about the nature and mass of the accretor.

2.1.1 Individual black-hole systems of Plotkin et al. (2013)

In Figure 2 we showed the average data for the black-hole X-ray transients from Plotkin et al. (2013). Such averaging might make potential outliers in the black-hole sample invisible. It could be possible that some systems have X-ray spectra considerably softer than the average (and thus possibly more consistent with the neutron-star systems than on average). Therefore, in Figure 4 we show the individual black-hole systems. Clearly this figure shows that, despite the larger errors and the scatter in the data points, none of the black-hole systems lies significantly above the average track. Therefore, we are convinced that using the average data points does not introduce biases.

2.2 Comparison with accreting millisecond X-ray pulsars

In Figure 5 we compare the three accreting millisecond X-ray pulsars for which we found appropriate data points in the literature with the non-pulsating systems. From this figure it appears that the pulsating systems are harder (at the same luminosities) than the non-pulsating systems. In particular the X-ray transient IGR J18245-2452 located in the globular cluster M28 is very hard (i.e., above 10^{36} erg s $^{-1}$; Linares et al. 2014), even harder than the black-hole systems³. This is contrary to the generally believed idea that black-hole systems are typically harder than the neutron-star ones. However, this source is on of the very few neutron-star X-ray transient that transits between an accreting millisecond X-ray pulsar when in outburst and a millisecond radio pulsar when in quiescence (Papitto et al. 2013). It is

³ The small errors on the column densities for this source, as reported in Table 3, strongly indicated that an underestimation of the column density could not have resulted in the very low photon indices measured. In addition, for the quoted luminosities the unresolved faint-source background in M28 does not affect the obtained spectral parameters (Linares et al. 2014)

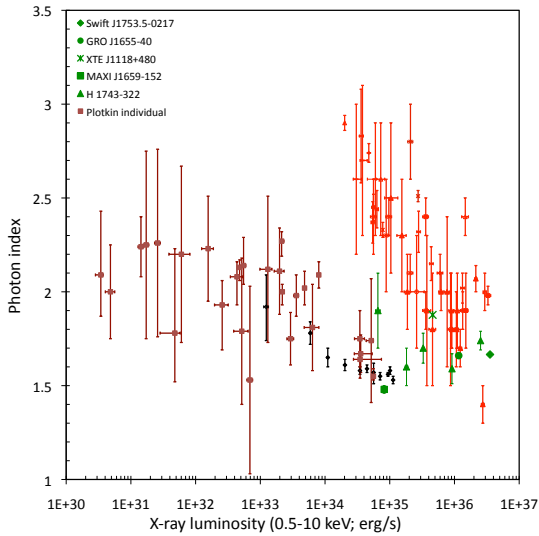


Figure 4. Similar to Figure 2 but with the black-hole systems from Plotkin et al. (2013) plotted as individual points. (A colour version of this figure is available in the online version of this paper.)

quite possible that its very hard spectra might be related to this unique character (although this would not remove the fact that some neutron-star X-ray transients can be harder than the black-hole systems). Moreover, the other AMXPs do not have such hard spectra when in outburst, although maybe the spectra might still be (slightly) harder than the non-pulsating systems.

We used again a 2D KS test to check whether the AMXP data were consistent with the data from the non-pulsating neutron-star systems applying the same method of section 2.1. We found a 90 % confidence interval for the probability that they are the same of 1.2×10^{-6} - 3.5×10^{-4} . However, since we only have three systems and IGR J18245–2452 might dominate the distribution for the AMXPs, we redid the KS test but now with this source removed. In that case, we found a probability interval of 4.8×10^{-3} - 3.6×10^{-1} that the AMXPs have the same distribution as the non-pulsating systems. This implies that we cannot draw any strong conclusions, especially given the fact that our AMXP sample is very limited. Therefore we cannot state conclusively that the presence of a dynamically important magnetic field alters the X-ray spectra of neutron-star LMXBs.

2.3 Below 10^{34} erg s $^{-1}$: quiescence

The black-hole systems we consider go to significantly lower luminosities than the neutron-star systems because for the black holes we did not apply the 10^{34} erg s $^{-1}$ cut-off criterion as we did for the neutron-star systems. When we include similarly low luminosities for the neutron-star systems, the situation becomes very complex: some systems are totally thermally dominated resulting in very large photon indices (3–5; e.g., Rutledge et al. 2001b, 2002b; Tomsick et al. 2004)

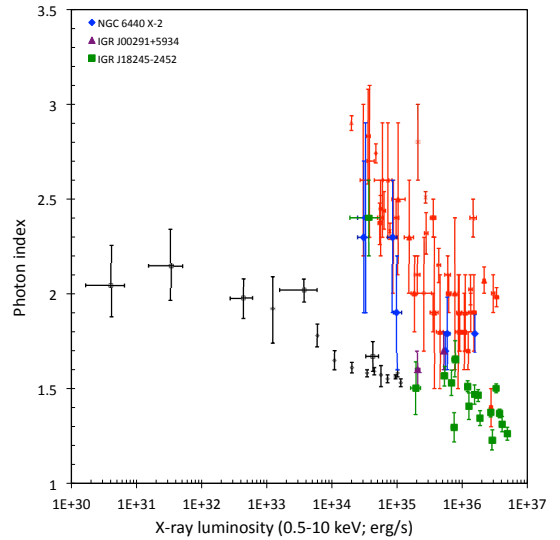


Figure 5. Adapted from Figure 1. The red points are the neutron-star systems and the black ones the black-hole binaries. Also included are the data points (green) for the transient and AMXP IGR J18245–2452 which is located in the globular cluster M28 and two other AMXPs (NGC 6440 X-2: blue; IGR J00291+5934: purple; a colour version of this figure is available in the online version of this paper).

but others are power-law dominated with photon indices as low as ~ 1.0 – 1.8 (e.g., Campana et al. 2002; Wijnands et al. 2005; Heinke et al. 2007, 2009; Degenaar et al. 2012e). The strong thermal emission could be due to residual accretion on the surface, but likely in many systems it is due to the cooling emission from the neutron star that has been heated during the outburst (e.g., Brown et al. 1998; Rutledge et al. 1999, 2001a,b; Campana et al. 2000). The power-law dominated spectra for quiescent neutron-star transients are not understood (see, e.g., the discussion in Campana et al. 1998) but the power-law component could be related to the fact that the neutron star has a magnetosphere (see Degenaar et al. 2012e, for a recent discussion). Because of these complications and the large range of photon indices in the neutron-star systems, we do not plot the neutron-star data for luminosities below 10^{34} erg s $^{-1}$. For black-hole systems, the situation is much cleaner since any effect on the spectra by a solid surface or a magnetic field is absent and all the X-rays should be due to some form of low-level accretion. This is reflected in the rather homogeneous behaviour of the black-hole systems in their quiescent state (see Plotkin et al. 2013, for a detailed discussion). It is interesting to note that at quiescent luminosities some neutron-star systems have significantly harder X-ray spectra than the black-hole transients (e.g., SAX J1808.4–3658, EXO 1745–248 Campana et al. 2002; Heinke et al. 2009; Degenaar & Wijnands 2012), although most of these hard systems (except EXO 1745–248) are accreting millisecond X-ray pulsars and their hard quiescent spectra might be related to the presence of a dynamically important magnetic field (see discussion in Degenaar et al. 2012e).

3 UNCERTAINTIES

The neutron-star points in Figure 1 display significant scatter, which could be intrinsic due to source differences. If true, then this would imply that although all sources become significantly softer at low luminosities, they might not all follow exactly the same uniform relation with decreasing luminosity. However, several types of systematic uncertainties are likely to be present in the data which would also give rise to significant scatter. Therefore a uniform relationship for all sources cannot be excluded at present. The main possible contributors to the scatter are discussed below. However, despite those uncertainties, we are convinced that the difference between the neutron-star systems and the black-hole ones in the luminosity range between 10^{34} and 10^{35} erg s^{-1} is robust.

3.1 The distance

For the neutron-star systems the distance is usually determined from the observation of type-I X-ray bursts, except for XTE J1719-291 and IGR J17494-3030 which so far have not displayed type-I X-ray bursts (we used for both sources a distance of 8 kpc because of their proximity to the Galactic centre; Table 1). Depending on the assumed burst properties (e.g., what type of fuel is burning on the surface and in which type of environment such as Hydrogen rich or Hydrogen poor) the obtained distances can vary by 50% or more. E.g., for AX J1754.2-2754 a distance of 6.6 or 9.2 kpc was obtained by Chelovekov & Grebenev (2007). In Figure 1 we used a distance of 9.2 kpc, but if the distance would be 6.6 kpc, the X-ray luminosity would decrease by a factor of ~ 2 . This would shift the source more in line with the other sources because now it has relatively soft photon indices for its luminosity compared to the majority of sources (Fig. 1). However, similar uncertainties exist in the distance measurements of the other sources, leading up to uncertainties in the X-ray luminosity of a factor 2 or 3. However, even if all neutron-star sources would shift down by this factor, they would still not be consistent with the black-hole ones. Moreover, for several sources we might have actually underestimated the distances instead of overestimating them, which would move some sources to higher luminosities and not lower luminosities, strengthening the difference between black-hole and neutron-star LMXBs.

We note that similar distance uncertainties exist in the black-hole data used by Plotkin et al. (2013). In addition, for Swift J1357.2-0933 we used a distance of 1.5 kpc. However, recently it has been argued that the distance for this source could range from 0.5 kpc up to 6.3 kpc (Shahbaz et al. 2013). Using this distance range would move the data down by a factor of up to 9, making the source exceptionally faint in outburst as well as in quiescence (Armas Padilla et al. 2014b), or up by a factor of up to 18, which still would make the system not consistent with the neutron-star systems.

3.2 Pile-up effects

Despite the low X-ray luminosities, the source fluxes can be still high enough to produce significant pile-up during some of the observations, especially if taken with *Chandra* in imaging mode (e.g., in 't Zand et al. 2005). The effect would

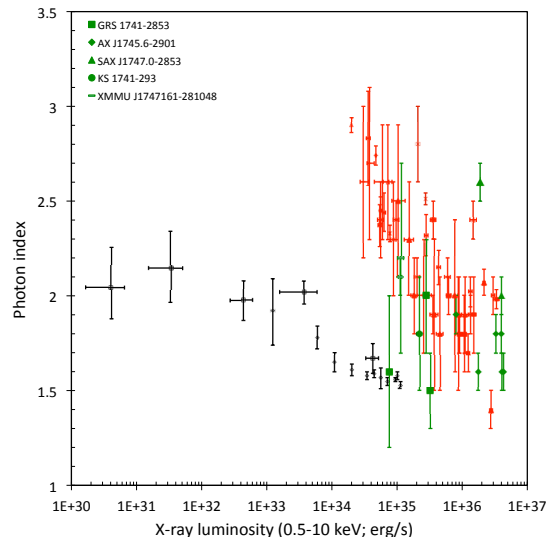


Figure 6. Adapted from Figure 1 but with the black holes displayed as the black points and the neutron stars as the red points. Also shown are several neutron-star transients which have very high column densities (the green points). (A colour version of this figure is available in the online version of this paper.)

be that the spectra would appear artificially harder than they really are. Since we found that the brightest sources have the hardest spectra, the question arises whether this could be due to pile-up effects. However, in our selection we did not include data points which are significantly affected by pile-up. Additionally, a lot of data were obtained using *XMM-Newton* or *Swift* which are less sensitive to pile-up and often the high-time resolution mode was used when the sources were relatively bright. Although we cannot exclude that some data points are still affected by a small amount of pile-up, most sources did not show evidence for pile-up (see, e.g., Armas Padilla et al. 2013b) so likely the effect of pile-up will be small and cannot explain the overall correlation we found.

3.3 Column density

Despite the fact that we do not use the neutron-star systems which have a $N_{\text{H}} > 5 \times 10^{22} \text{ cm}^{-2}$, the range in N_{H} is still large (ranging from $0.2 \times 10^{22} \text{ cm}^{-2}$ to $\sim 3 \times 10^{22} \text{ cm}^{-2}$; Tab. 1). This range might still produce a systematic effect on the photon indices since it is well known that when fitting a power-law model to relatively poor quality data, a strong correlation will be found between the photon index and the column density (see, e.g., the detailed study performed on faint black-hole systems by Plotkin et al. 2013). However, we would like to stress here that for the few sources in our sample that have a high dynamic range in luminosities, that they individually showed this softening with decreasing luminosities (see, e.g., Armas Padilla et al. 2011; Bahramian et al. 2014; Linares et al. 2014). For those sources the systematic

effects of using an incorrect column density should be minimal.

For the complete sample, any systematic effect from obtaining an incorrect column density should be reflected in the errors on the photon indices. However, on several occasions the column density was frozen to an assumed value (e.g., the expected Galactic column density towards the source or the value obtained during higher quality data sets from the sources). If the wrong value is assumed, this would skew the photon index to higher or lower values than the true one and introduce scatter in the diagram, although it is currently not clear how much scatter this would produce. A detailed study of this is beyond the scope of this paper.

When including those sources that have very high column densities ($> 5 \times 10^{22} \text{ cm}^{-2}$), most of those sources are consistent with the other neutron-star data points (Figure 6) although there seems to be some indications that at the same luminosity (below $10^{36} \text{ erg s}^{-1}$) the highly absorbed sources have a smaller photon index compared with that observed for the low- N_{H} sources. We performed a 2D KS test between the data points for systems with a low column density and those that have a high column density. The result is a 90 % confidence interval for the probability that they are drawn from the same distribution of $8.7 \times 10^{-4} - 6.4 \times 10^{-2}$. Although this result might indicate that their distributions could be different, the low column density data set goes to significantly lower luminosities than the high column density data set. Therefore, we performed also a 2D KS test between the two data sets but limiting the low column density data points to the same luminosity range as the high column density ones (i.e., from luminosities $> 7 \times 10^{34} \text{ erg s}^{-1}$). The resulting 90% confidence interval increases to $4.5 \times 10^{-3} - 1.7 \times 10^{-1}$, indicating that it is less likely that the two data sets are drawn from different distributions. However, given the limited amount of data points, we cannot make a strong conclusion. Moreover, as we will argue in section 4.1, the softening is likely due to the neutron-star surface becoming prominently visible at low energies. Therefore the softening concentrates at low energies in the X-ray spectra where also the absorption affects the spectra the most. As a consequence the highly absorbed sources will show less apparent softening than the less absorbed systems and any possible difference is therefore likely not physical.

3.4 Calculating the 0.5-10 keV luminosities and its errors

Not all publications we used quoted the luminosities or unabsorbed fluxes in the 0.5–10 keV band. Some publications quoted only the 2–10 keV or the 0.3–10 keV luminosities. We used WebPIMMS⁴ to calculate the luminosities in the 0.5–10 keV energy range, but this introduces additional uncertainties since extrapolation outside the specified energy range may not be valid. In addition, in some publications the luminosities or fluxes are reported but not their uncertainties (see Tab. 1); in such cases we assumed an error of 10% on the fluxes, although this is likely an underestimation of the true errors. However, both types of uncertainties will likely

have only a small effect on the observed correlation seen in Figure 1 because the scatter in X-ray luminosity is dominated by the uncertainties in the distances which typically result in luminosity uncertainties of a factor of a few (see discussion in section 3.1).

3.5 Complex spectral shape

When the data have low statistics, a single power-law model can adequately fit the X-ray spectra, but for high quality data a single power-law model often does not provide a good fit. Adding a second (often assumed to be thermal) component is required. Moreover, in the discussion section we will argue that in most, if not all, neutron-star systems, a soft thermal component might be present at the lowest luminosities even if it cannot be detected due to the limitation of the data. To obtain a homogenous data sample, we have still included the results obtained using a single power-law model of those sources for which indeed such a soft component is clearly needed to fit the spectra accurately. By doing so possible systematic effects might have been introduced. However, likely they are not very significant because when low (e.g., *Swift*) and high (e.g., *XMM-Newton*) quality data are available for the same source at roughly the same X-ray luminosities, the photon indices (when fitting a single power-law model) obtained from the different data sets are fully consistent with each other (see, e.g., Armas Padilla et al. 2011).

3.6 The effect of individual sources

Since we are interested in the average behaviour of our sample, it is possible that individual sources might not follow exactly the correlation found for the total sample of sources. For example, the black-hole point in Figure 2 that has luminosity of $\sim 5 \times 10^{35} \text{ ergs}^{-1}$ but a relatively large photon index of ~ 1.88 is the only available point of XTE J1118+480 (Reis et al. 2010). Excluding this point would cause the black-hole points in Figure 2 to overlap less with the neutron-star data for luminosities $> 10^{35} \text{ erg s}^{-1}$. Therefore, excluding this point would strengthen the conclusion that neutron-star systems are softer than black-hole transients. And indeed arguments can be put forward to exclude this point because it was obtained from high quality data taken with the *Chandra*/LETG instrument which is particularly sensitive at low energies. Furthermore, the X-ray spectra were only fitted up to $\sim 7 \text{ keV}$ (due to the instrument response) making the lower energies more dominant in the spectral fits. This, in combination with the very low column density of this source and the clear presence of a soft component in the spectrum (likely due to the accretion disc, see Reis et al. 2009), might have artificially skewed the photon index to high values. However, since it is unclear what photon index would have been obtained for the source if the data quality was lower and the absorption higher, we still include this data point in our figure. Although in this work we aim to describe the general behaviour rather than explaining individual sources, it is clear that individual sources might behave (slightly) differently compared to the majority of sources.

⁴ Available at <http://heasarc.gsfc.nasa.gov/Tools/w3pimms.html>

4 DISCUSSION

We searched the literature for reports on the spectral properties of neutron-star LMXBs when they have accretion luminosities between 10^{34} and 10^{36} ergs s^{-1} , corresponding to roughly 0.01% to 1% of the Eddington mass accretion rate (\dot{M}_{Edd}). Despite the variety of models fitted to the X-ray spectra, for many systems the results were reported from fits that used a simple absorbed power-law model. When plotting the photon index versus the luminosity (Fig. 1) a clear trend is visible: the photon index increases (thus the spectra become softer) with decreasing luminosities. Such behaviour has been reported before for individual neutron-star LMXBs (e.g., see Degenaar et al. 2013; Armas Padilla et al. 2011, 2013b,c, and references therein), but here we demonstrate that very likely most neutron-star systems behave in a similar manner and they might even follow a universal relation.

When comparing the neutron-star systems with the averaged points reported by Plotkin et al. (2013) for a collection of black hole systems (10 sources) and with the specific black-hole transient Swift J1357.2–0933 (Armas Padilla et al. 2013a), it is clear that the black holes are significantly harder at luminosities below 10^{35} erg s^{-1} . Not enough black-hole systems are available in the luminosity range 10^{35} to 10^{36} erg s^{-1} to make conclusive statements for this range. Although the black-hole transients observed in this luminosity range are on average harder than the neutron-star systems, there is significant overlap between the two source classes *and* the hardest source (IGR J18245–2452; Linares et al. 2014) in our sample is in fact a neutron-star LMXB and not a black-hole system.

Similar to the neutron-star systems, at low luminosities the black-hole binaries also become softer, but this softening occurs at significantly lower luminosities (around 10^{34} erg s^{-1} ; see also the discussions in Armas Padilla et al. 2013a; Plotkin et al. 2013) than what we observe for the neutron-star systems for which the softening already starts at 10^{36} erg s^{-1} . In addition, the black holes seem to level off at a photon index ~ 2 , but the neutron-star systems reach photon indices of 2.5–3. Neutron-star systems at even lower luminosities (below 10^{34} erg s^{-1} ; i.e., when they are in quiescence) display a large variety of behaviour (see section 2.3) and are therefore not studied in this work.

4.1 Origin of the softening of the neutron-star systems

When high quality data is available of the neutron-star systems at X-ray luminosities in the range 10^{34} to 10^{35} erg s^{-1} , typically a soft component needs to be added to the power-law model to obtain an acceptable fit (e.g., Armas Padilla et al. 2013b; Degenaar et al. 2013). It also has been found that when the X-ray luminosity decreases for certain sources, the temperature of this soft component decreases. The soft component and the decrease in temperature have been interpreted (Degenaar et al. 2013; Armas Padilla et al. 2013c; Bahramian et al. 2014) as the neutron-star surface becoming clearly visible in the X-ray spectra originating from low-level accretion onto the neutron-star surface. The decrease in luminosity is then due to a decrease in accretion rate onto the surface causing the surface temperature to go down.

Interestingly, when a soft component is added to the spectral model, the power-law component suddenly becomes significantly harder with a photon index well below 2 (e.g., Degenaar et al. 2012d; Armas Padilla et al. 2013b; Degenaar et al. 2013, we note that the errors on the photon indices are typically large but the general trend is that the power-law component is rather hard). This might suggest that the softening of the overall spectrum is due to the neutron-star surface becoming more and more dominant in the X-ray spectra. However, at luminosities above 10^{35} erg s^{-1} , a soft component is not always needed to fit the spectra adequately (Armas Padilla et al. 2013b). In addition, the photon indices are relatively high already irrespectively of whether or not a soft component is included in the spectral fits.

Taking the above observational facts into account, we propose two possible phenomenological scenarios (see also the discussion in Armas Padilla et al. 2013b) that might be able to explain the softening of the neutron-star spectra when the luminosity decreases from 10^{36} erg s^{-1} to 10^{34} erg s^{-1} . These different scenarios are illustrated in Figure 7. In scenario 1, the power-law component (assumed to be due to the accretion process) starts out with a relatively hard index (< 2 ; the source is in the so-called hard state or extreme island state for neutron-star LMXBs) for luminosities above 10^{36} erg s^{-1} (note that this luminosity range is not shown in Fig 7, which starts at 10^{36} erg s^{-1}). When the luminosity decreases to $\sim 10^{35}$ erg s^{-1} , the photon index becomes larger (increasing to a value of > 2 ; left panel of scenario 1 in Fig. 7) resulting in an overall softening of the spectrum. The thermal component (assumed to be due to low-level accretion onto the neutron-star surface) is either still absent or only weakly detectable in the X-ray spectra and does not contribute to the softening of the overall spectrum. Then, at luminosities below 10^{35} erg s^{-1} the power-law component becomes suddenly harder again (with a photon index well below 2 again; two right panels of scenario 1 in Fig. 7). At the same time the thermal component becomes a major component in the X-ray spectra and since its temperature is going down with decreasing luminosity, the resulting overall spectrum softens further.

In scenario 2, the source started out in a similar state as in scenario 1, with a hard power-law component at a luminosity of 10^{36} erg s^{-1} . Also in this scenario the power-law component (labelled a) softens when the luminosity decreases to 10^{35} erg s^{-1} but around this luminosity the soft component might become visible in the spectra *together* with an extra harder power-law component (with a photon index well below 2; labelled b in Fig. 7, left panel) whose origin is not known at the moment. Due to the usually poor quality of the obtained data, the components are typically difficult to separate from each other and when fitting the data with a single power-law model, the overall spectrum is rather soft with a high photon index (> 2). When the luminosity decreases further, the power-law component (power law a) due to the accretion flow decreases in strength. Although this component could possibly soften further, at this time the thermal emission from the neutron-star surface and the second, harder power-law component (power law b) dominate the spectrum. At the lowest luminosities of $\sim 10^{34}$ erg s^{-1} , the original power-law component (power law a) has decayed to very low flux levels and cannot be detected any-

more in the spectra. Only the thermal component and the hard power-law component (power law b) are detected. The softening of the X-ray spectra is mostly due to a decrease of the temperature of the thermal component.

Although it is currently unclear which scenario is the correct one (or that it could be a combination of both scenarios), we currently consider scenario 2 as the most promising one. In black-hole systems the power-law component *must* come from the accretion process and it is now well established that at the lowest accretion luminosities this component becomes softer (see discussion in Plotkin et al. 2013). Considering the many similarities in the accretion process between neutron-star systems and the black-hole ones, it is reasonable to assume that the power-law component will behave similarly in both types of systems. The softening can be explained in context of radiatively inefficient accretion flows (see the discussions in Armas Padilla et al. 2013a; Plotkin et al. 2013, and references therein). In this model, it is difficult to understand why in the neutron-star systems the spectra should be harder than in the black-hole binaries when both systems are in quiescence. We consider it more plausible that not one but two processes are active at low accretion rates in the neutron-star systems which both produce a power-law component in the spectrum. One process is tied to the accretion flow at large distances and one is due to an unknown origin (in section 4.2 we discuss the possible nature of this component further). High signal-to-noise ratio observations at the right X-ray luminosity are needed to be able to distinguish between the two scenarios.

When the luminosity decreases even further (to quiescent luminosities) for the neutron-star systems, three different possibilities can be observed (see Fig. 7). First, some systems are totally dominated by a power-law component (Fig. 7 right bottom). It is currently still unclear what causes this component (it has been postulated that it might be related to the magnetic field of the neutron star; see the discussions in Campana et al. 1998; Rutledge et al. 2001b; Degenaar et al. 2012e) and if it is related to the power-law component (scenario 1) or components (scenario 2) seen at higher luminosities. Second, some quiescent X-ray spectra could be totally dominated by a thermal component (Fig. 7 right middle). Typically it is assumed that this is due to cooling emission from the neutron star which has been heated during outburst (e.g., Brown et al. 1998; Rutledge et al. 1999, 2001a,b; Campana et al. 2000), although very low level accretion onto the neutron-star surface cannot be excluded either. Third, in some quiescent sources both spectral components are still clearly detectable. Usually, the power-law component is hard with photon indices well below 2 (and sometimes even below 1, although the errors are typically very large). Although the soft component could be due to cooling of the neutron star, variability in this component in some neutron-star X-ray transients in quiescence (e.g., Cen X-4, Aql X-1 Campana et al. 1997, 2004; Rutledge et al. 2002a; Cackett et al. 2010, 2011, 2013; Bernardini et al. 2013) suggests that very low-level accretion onto the neutron-star surface is more likely in those systems. Since the spectral shape (i.e., a two component model with a hard power-law component) of these quiescent neutron stars is very similar to that of the neutron-star LMXBs at $\sim 10^{34}$ erg s $^{-1}$, we tentatively suggest that the underlying physical mechanism is the same. The lower temperature of neutron-

star surfaces in the quiescent systems compared to those at higher luminosities can be explained because of the lower accretion rate onto the surface of the neutron stars. The hard component still remains an enigma, but in the next section we suggest that it might be directly connected with the accretion process onto the surface as well.

This suggestion is further supported by the very recent paper by D’Angelo et al. (2015) which studied the quiescent spectrum of the neutron-star X-ray transient Cen X-4. They also reached the conclusion that in this source both the thermal as well as the non-thermal component are due to low level accretion onto the neutron-star surface. This conclusion is consistent with our conclusions, although we suggest that this is true not only for the quiescent systems but also for the sources that have X-ray luminosities up to a few times 10^{34} erg s $^{-1}$.

4.2 A roughly equal contribution of the soft and hard component to the 0.5–10 keV luminosity?

When both the soft and the hard component are clearly distinguished in the X-ray spectrum, one can calculate the relative contribution of both components to the 0.5–10 keV luminosity. This has been done for several sources, both actively accreting sources (Armas Padilla et al. 2013b; Campana et al. 2014) and quiescent systems (Cackett et al. 2010; Fridriksson et al. 2011; Homan et al. 2014). When looking at those references, it becomes strikingly apparent that when there are good indications that the source is actively accreting onto the surface of the neutron star⁵ in many occasions both components contribute about half⁶ the flux in the 0.5–10 keV energy range (within the, often large, errors).

Moreover, for Cen X-4 there are many quiescent observations at different flux levels and both components increase and decrease in a similar fashion, ensuring that the contribution of both components to the 0.5–10 keV flux remains about equal (Cackett et al. 2010). In addition, Campana et al. (2014) reported for Aql X-1 that the fractional contribution of both components remained roughly constant (for luminosities below 10^{35} erg s $^{-1}$; above that the power-law component dominated fully the X-ray spectra) when it was decaying after a main outburst. Only at the lowest luminosities (a few times 10^{33} erg s $^{-1}$) the thermal component dominated (although the power-law contribution was still of order 30%; at these luminosities it was proposed by Campana et al. (2014) that the source was in the cooling regime and that the neutron star was not accreting anymore). Finally, Bahramian et al. (2014) found that during the rise of the third discovered X-ray transient in the globular cluster Terzan 5, the soft component and the hard component also increased together in such a way that their fractional contributions to the 0.5–10 keV luminosity

⁵ This would be because type-I X-ray bursts are observed or strong variability is observed either during the observation or between different observations (e.g., accretion flares on top of a crust cooling curve Fridriksson et al. 2011; Homan et al. 2014)

⁶ With ‘about half’ we mean that the contribution of the different components always lay within 40% to 60% of the total flux.

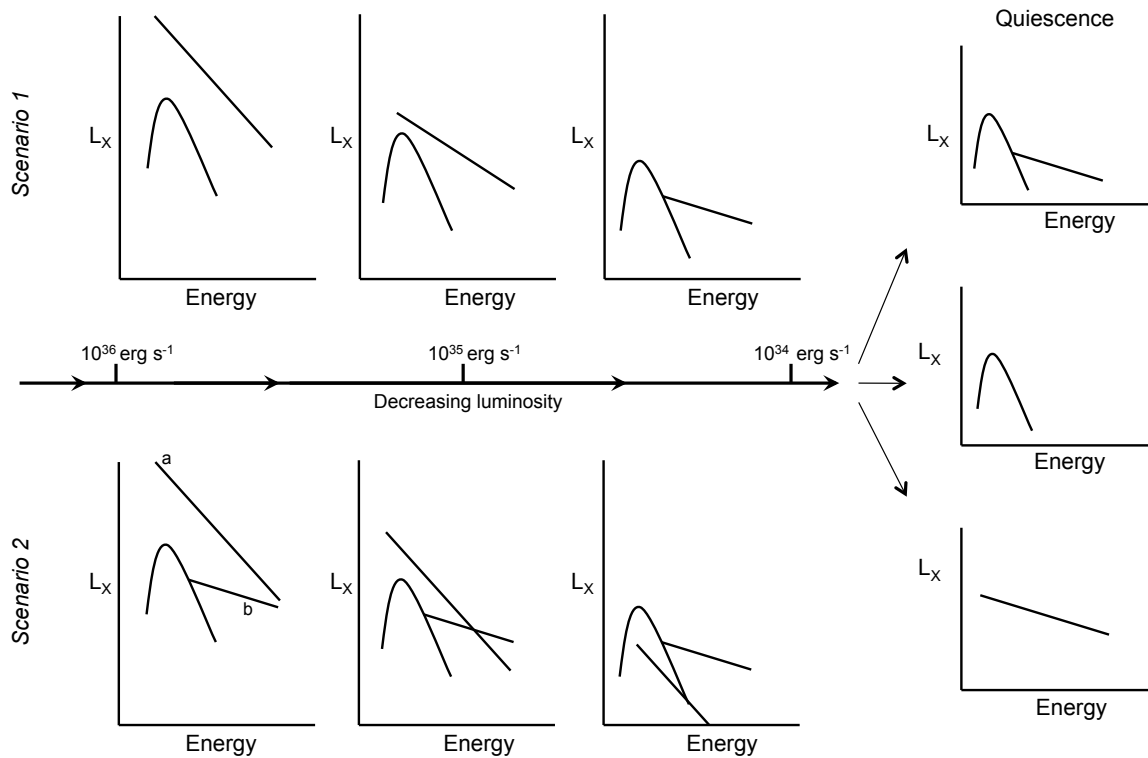


Figure 7. Two possible scenarios explaining the observed softening of the neutron-star spectra when the X-ray luminosity decreases from $10^{36} \text{ erg s}^{-1}$ down to $10^{34} \text{ erg s}^{-1}$ (see main text for full details). In quiescence (right panels) three different type of quiescence spectra are observed: the spectrum is fully dominated by the power-law component (bottom), the spectrum is fully dominated by the thermal component (middle) or in the spectrum both components are clearly detected (top).

remained approximately 50%. Only above a luminosity of $\sim 10^{35} \text{ erg s}^{-1}$ this broke down and the power-law component became much more dominant than the thermal component (see their Table 4).

This all indicates that some fundamental physical process is occurring at low accretion rates in neutron-star systems that causes the physical mechanism behind the hard component to be connected with that behind the soft component. Only above a luminosity of $\sim 10^{35} \text{ erg s}^{-1}$ this might not be true anymore since the power-law component then dominates the X-ray spectra. At quiescent luminosities ($< 10^{34} \text{ erg s}^{-1}$) it depends on the contribution of the thermal component due to the cooling of the neutron star, which physical process dominates the X-ray emission. It is interesting to note that in the most basic disc theory for accretion onto neutron stars (Frank et al. 2002), half the luminosity is generated in the accretion disc and the other half when the matter hits the surface. Although it is likely that no disc is present close to the neutron stars when they are at very low luminosities, it is possible that the energy stored in the accretion flow is released in such a way that half of it

is emitted very close to the neutron star and the remainder when the matter hits the star.

Only a few authors have modelled low level accretion onto neutron stars (see for example the discussions in Rutledge et al. 2002b; Bahramian et al. 2014). Zampieri et al. (1995) found that the resulting X-ray spectrum would be harder than a simple black-body spectrum, but no significant hard tail would be present. Similar conclusions were reached by other authors although some studies found that a (relatively weak) power-law component was also present (e.g., Deufel et al. 2001). More detailed theoretical investigations are needed to determine the exact emerging spectra of low-level accretion onto neutron stars, but if our hypothesis is correct the hard power-law component also have to be explained by such models and that it should contribute about half to the 0.5–10 keV luminosity.

4.3 Comparing with Jonker et al. (2004a,b)

Jonker et al. (2004a,b) found that for quiescent neutron-star systems there appears to be an anticorrelation between the

fractional power-law contribution and the total 0.5–10 keV luminosity for systems that are fainter than $\sim 2 \times 10^{33}$ erg s⁻¹ and a correlation between those contributions for systems that are brighter than this luminosity. From Figure 5 in Jonker et al. (2004b) it can be seen that they have data points for only one source that has luminosities above 10^{34} erg s⁻¹ (i.e., XTE J1706–267). Consistent with what we discussed in section 4.2, that source has a fractional contribution of the power-law component of $\sim 50\%$. The reason why, when the luminosity decreases below 10^{34} erg s⁻¹, the fractional contribution of the power-law component decreases is likely that the thermal emission will be dominated by cooling emission from the neutron-star surface and not by the accretion emission. If true, then the exact relation might be different for different sources since the temperature of the neutron-star surface is likely not the same for all sources because of their different accretion histories. The emergence of a dominating power-law component below 2×10^{33} erg s⁻¹ might suggest that at the lowest luminosity a different power-law component appears (as suggested as one of the possibilities in section 4.2), whose origin is still unclear.

4.4 A diagnostic tool to separate the neutron-star systems from the black-hole ones?

The strong indication that most neutron-star LMXBs are significantly softer than black-hole systems below an X-ray luminosity of 10^{35} erg s⁻¹ (and possibly 10^{36} erg s⁻¹, but at this luminosity the source classes overlap) suggests that we can use the rough spectral shape between 0.5 and 10 keV as a diagnostic tool to separate the neutron-star LMXBs from the black-hole systems. For example, for both IGR J17494–3030 and XTE J1719–291 it has not conclusively been determined that they are neutron-star systems since no type-I X-ray bursts or X-ray pulsations were observed. However, it has been argued that they are strong candidate neutron-star LMXBs (Armas Padilla et al. 2011, 2013c). Indeed, the spectral index obtained when fitting their spectra with a simple power-law model falls right in the regime of the confirmed neutron-star LMXBs⁷.

Similarly, Sidoli et al. (2011) reported on the X-ray spectral properties of the unclassified X-ray transient IGR J17285–2922 (also called XTE J1728–295). From the low X-ray upper limit on the quiescent luminosity of the source, they suggested it likely harbours a black hole as compact primary, but they could not be conclusive. However, they also reported that the photon index was 1.61 ± 0.01 when the source had a X-ray luminosity of $\sim 6.1 \times 10^{35}$ erg s⁻¹ (0.5–10 keV; converted from the listed 0.3–10 keV flux using WebPIMSS, and assuming a distance of 8 kpc). This would place the source just below the neutron-star points in Figure 1 but fully consistent with the black-hole points. Although the neutron-star transient IGR J18245–2452 in the globular cluster M28 has similar hard spectra at this luminosity (Linares et al. 2014), this behaviour is more commonly observed for black-hole systems. So, although we cannot conclusively determine the nature of the compact object

in this system, this would add evidence to the suggestion by Sidoli et al. (2011) that this source harbours a black hole.

Another interesting source is AX J1548.3–5541. Degenaar et al. (2012a) suggested that it is likely a LMXB. Its X-ray spectrum is too soft (with a photon index of 2.3 ± 0.1) for it to be a high-mass X-ray binary. These authors could not say anything about the nature of the accretor if the source is truly a LMXB. In their paper, they reported the luminosity in the 0.3–10 keV band and when we convert that (using WebPIMMS) to 0.5–10 keV we get a luminosity of $\sim 3 \times 10^{35}$ erg s⁻¹. These luminosity and photon index would place the source right on the neutron-star track in Figure 1 and therefore, we tentatively classify this source as a neutron-star LMXB.

Another unclassified source is the X-ray transient XMMSL1 J171900.4–353217 (see Read et al. 2010a,b; Markwardt et al. 2010). Armas Padilla et al. (2010) and Read et al. (2010b) reported on the spectral properties of this source and they found a relatively soft X-ray spectrum (with photon index > 2). If we assume a fiducial distance of 8 kpc for this source, its X-ray luminosity is typically around 10^{35} erg s⁻¹ (Read et al. 2010b; Armas Padilla et al. 2010). This would put the source right on the neutron-star track and well above that observed for the black-hole systems. Therefore, we also tentatively identify this source as a neutron-star LMXB.

A very peculiar source is the X-ray transient IGR J17361–4441 located in the globular cluster NGC 6388 (Gibaud et al. 2011; Ferrigno et al. 2011). The nature of this source remains an enigma. Its transient behaviour, and location in a globular cluster would suggest the source being a LMXB. However, its very hard X-ray spectra (with photon indices ~ 1 ; Ferrigno et al. 2011; Wijnands et al. 2011; Bozzo et al. 2011) are not consistent with the typically observed spectra of LMXBs at the luminosities observed for the source (peak luminosities of 6 to 9×10^{35} erg s⁻¹; Wijnands et al. 2011). Alternative explanations have been put forward (Wijnands et al. 2011; Del Santo et al. 2014), but in the appendix we argue that the source is indeed a LMXB harbouring either a black hole or a low-magnetic field neutron star. However, comparing IGR J17361–4441 with the other sources shown in Figure 1 demonstrates that it is not consistent with either the neutron-star systems or with the black-hole transients. Therefore, some unusual systems behave differently than the average population and are not classifiable using Figure 1.

To conclude, we propose that comparing the spectral index obtained from fits with a simple power-law model at a 0.5–10 keV luminosity of $10^{34} - 10^{35}$ erg s⁻¹ (Fig. 1) can be used to suggest in most circumstances (but not all, as we demonstrated above using IGR J17361–4441) the nature of the compact object in an unclassified X-ray binary, if this source exhibits accretion luminosities between 10^{34} and 10^{35} erg s⁻¹. More systems need to be studied in this luminosity range to confirm that Figure 1 can indeed be used as a diagnostic tool. In addition, more systems have to be studied between 10^{35} and 10^{36} erg s⁻¹ to determine if also in this luminosity range neutron-star LMXBs have (on average) softer spectra than the black-hole systems.

⁷ We note that if we remove both sources from our plots, the correlation we found does not change so the effect of those sources on our correlation is minimal.

Acknowledgements

RW and MAP acknowledge support from a European Research Council (ERC) starting grant awarded to RW. ND acknowledges support via an EU Marie Curie Intra-European fellowship under contract no. FP-PEOPLE-2013-IEF-627148. MAP is supported by Canary Island CIE: Tri-continental Atlantic Campus. DA acknowledges support from the Royal Society. COH is supported by an NSERC Discovery Grant and an Ingenuity New Faculty Award and an Alexander von Humboldt Fellowship. RW thanks Caroline D'Angelo for useful discussion and for receiving her manuscript before submission. This research has made use of NASA's Astrophysics Data System.

REFERENCES

- Allen, J. L., Linares, M., Homan, J., & Chakrabarty, D. 2015, *ApJ*, 801, 10
- Armas Padilla, M., Kaur, R., Degenaar, N., et al. 2010, *The Astronomer's Telegram*, 2722, 1
- Armas Padilla, M., Degenaar, N., Patruno, A., et al. 2011, *MNRAS*, 417, 659
- Armas Padilla, M., Degenaar, N., Russell, D. M., & Wijnands, R. 2013a, *MNRAS*, 428, 3083
- Armas Padilla, M., Degenaar, N., & Wijnands, R. 2013b, *MNRAS*, 434, 1586
- Armas Padilla, M., Wijnands, R., & Degenaar, N. 2013c, *MNRAS*, 436, L89
- Armas Padilla, M., Wijnands, R., Altamirano, D., et al. 2014a, *MNRAS*, 439, 3908
- Armas Padilla, M., Wijnands, R., Degenaar, N., et al. 2014b, *MNRAS*, 444, 902
- Bahramian, A., Heinke, C. O., Sivakoff, G. R., et al. 2014, *ApJ*, 780, 127
- Becker, R. H., Boldt, E. A., Holt, S. S., et al. 1977, *ApJ*, 214, 879
- Belloni, T., & Hasinger, G. 1990, *A&A*, 230, 103
- Bernardini, F., Cackett, E. M., Brown, E. F., et al. 2013, *MNRAS*, 436, 2465
- Bozzo, E., Ferrigno, C., Stevens, J., et al. 2011, *A&A*, 535, L1
- Bozzo, E., Papitto, A., Ferrigno, C., & Belloni, T. M. 2014, *A&A*, 570, L2
- Brown, E. F., Bildsten, L., & Rutledge, R. E. 1998, *ApJL*, 504, L95
- Cackett, E. M., Brown, E. F., Miller, J. M., & Wijnands, R. 2010, *ApJ*, 720, 1325
- Cackett, E. M., Fridriksson, J. K., Homan, J., Miller, J. M., & Wijnands, R. 2011, *MNRAS*, 414, 3006
- Cackett, E. M., Brown, E. F., Degenaar, N., et al. 2013, *MNRAS*, 433, 1362
- Campana, S. 2009, *ApJ*, 699, 1144
- Campana, S., Mereghetti, S., Stella, L., & Colpi, M. 1997, *A&A*, 324, 941
- Campana, S., Colpi, M., Mereghetti, S., Stella, L., & Tavani, M. 1998, *A&AR*, 8, 279
- Campana, S., Stella, L., Mereghetti, S., & Cremonesi, D. 2000, *A&A*, 358, 583
- Campana, S., Stella, L., Gastaldello, F., et al. 2002, *ApJL*, 575, L15
- Campana, S., Israel, G. L., Stella, L., Gastaldello, F., & Mereghetti, S. 2004, *ApJ*, 601, 474
- Campana, S., Stella, L., & Kennea, J. A. 2008, *ApJL*, 684, L99
- Campana, S., Brivio, F., Degenaar, N., et al. 2014, *MNRAS*, 441, 1984
- Casella, P., Altamirano, D., Patruno, A., Wijnands, R., & van der Klis, M. 2008, *ApJL*, 674, L41
- Chakrabarty, D. 1998, *ApJ*, 492, 342
- Chakrabarty, D., Tomsick, J. A., Grefenstette, B. W., et al. 2014, *ApJ*, 797, 92
- Chelovekov, I. V., & Grebenev, S. A. 2007, *Astronomy Letters*, 33, 807
- D'Angelo, C. R., Fridriksson, J. K., Messenger, C., & Patruno, A. 2015, *MNRAS*, 449, 2803
- Degenaar, N., & Wijnands, R. 2008, *The Astronomer's Telegram*, 1831, 1
- Degenaar, N., & Wijnands, R. 2009, *A&A*, 495, 547
- Degenaar, N., & Wijnands, R. 2010, *A&A*, 524, A69
- Degenaar, N., & Wijnands, R. 2012, *MNRAS*, 422, 581
- Degenaar, N., & Wijnands, R. 2013, *IAU Symposium*, 290, 113
- Degenaar, N., Wijnands, R., & Kaur, R. 2011, *MNRAS*, 414, L104
- Degenaar, N., Starling, R. L. C., Evans, P. A., et al. 2012a, *A&A*, 540, A22
- Degenaar, N., Wijnands, R., Cackett, E. M., et al. 2012b, *A&A*, 545, A49
- Degenaar, N., Altamirano, D., & Wijnands, R. 2012c, *The Astronomer's Telegram*, 4219, 1
- Degenaar, N., Linares, M., Altamirano, D., & Wijnands, R. 2012d, *ApJ*, 759, 8
- Degenaar, N., Patruno, A., & Wijnands, R. 2012e, *ApJ*, 756, 148
- Degenaar, N., Wijnands, R., & Miller, J. M. 2013, *ApJL*, 767, L31
- Del Santo, M., Sidoli, L., Mereghetti, S., et al. 2007, *A&A*, 468, L17
- Del Santo, M., Nucita, A. A., Lodato, G., et al. 2014, *MNRAS*, 444, 93
- Deufel, B., Dullemond, C. P., & Spruit, H. C. 2001, *A&A*, 377, 955
- Falanga, M., Belloni, T., & Campana, S. 2006, *A&A*, 456, L5
- Fasano, G., & Franceschini, A. 1987, *MNRAS*, 225, 155
- Ferrigno, C., Bozzo, E., Rodriguez, J., & Gibaud, L. 2011, *The Astronomer's Telegram*, 3566, 1
- Frank, J., King, A., & Raine, D. J. 2002, *Accretion Power in Astrophysics*, by Juhan Frank and Andrew King and Derek Raine, pp. 398. ISBN 0521620538. Cambridge, UK: Cambridge University Press, February 2002.,
- Fridriksson, J. K., Homan, J., Wijnands, R., et al. 2010, *ApJ*, 714, 270
- Fridriksson, J. K., Homan, J., Wijnands, R., et al. 2011, *ApJ*, 736, 162
- Gandhi, P., Dhillon, V.S., Tomsick, J.A., et al. 2014, *The Astronomer's Telegram*, 6447, 1
- Gibaud, L., Bazzano, A., Bozzo, E., et al. 2011, *The Astronomer's Telegram*, 3565, 1
- Giles, A. B., Swank, J. H., Jahoda, K., et al. 1996, *ApJL*, 469, L25
- Heinke, C. O., Jonker, P. G., Wijnands, R., & Taam, R. E.

- 2007, *ApJ*, 660, 1424
- Heinke, C. O., Jonker, P. G., Wijnands, R., Deloye, C. J., & Taam, R. E. 2009, *ApJ*, 691, 1035
- Heinke, C. O., Altamirano, D., Cohn, H. N., et al. 2010, *ApJ*, 714, 894
- Homan, J., Fridriksson, J. K., Jonker, P. G., et al. 2013, *ApJ*, 775, 9
- Homan, J., Fridriksson, J. K., Wijnands, R., et al. 2014, *ApJ*, 795, 131
- in 't Zand, J. J. M., Cornelisse, R., & Méndez, M. 2005, *A&A*, 440, 287
- in 't Zand, J. J. M., Jonker, P. G., Bassa, C. G., Markwardt, C. B., & Levine, A. M. 2009, *A&A*, 506, 857
- James, M., Paul, B., Devasia, J., & Indulekha, K. 2010, *MNRAS*, 407, 285
- James, M., Paul, B., Devasia, J., & Indulekha, K. 2011, *MNRAS*, 410, 1489
- Jonker, P. G., Wijnands, R., & van der Klis, M. 2004a, *MNRAS*, 349, 94
- Jonker, P. G., Galloway, D. K., McClintock, J. E., et al. 2004b, *MNRAS*, 354, 666
- Jonker, P. G., Miller-Jones, J., Homan, J., et al. 2010, *MNRAS*, 401, 1255
- Jonker, P. G., Miller-Jones, J. C. A., Homan, J., et al. 2012, *MNRAS*, 423, 3308
- Lewis, F., Russell, D. M., Jonker, P. G., et al. 2010, *A&A*, 517, A72
- Lin, D., Remillard, R. A., & Homan, J. 2007, *ApJ*, 667, 1073
- Linares, M., van der Klis, M., & Wijnands, R. 2007, *ApJ*, 660, 595
- Linares, M., Bahramian, A., Heinke, C., et al. 2014, *MNRAS*, 438, 251
- Lowell, A. W., Tomsick, J. A., Heinke, C. O., et al. 2012, *ApJ*, 749, 111
- Lü, G.-L., Zhu, C.-H., Postnov, K. A., et al. 2012, *MNRAS*, 424, 2265
- Markwardt, C. B., Strohmayer, T. E., & Swank, J. H. 2010, *The Astronomer's Telegram*, 2615, 1
- Menou, K., Esin, A. A., Narayan, R., et al. 1999, *ApJ*, 520, 276
- Miller, J. M., Raymond, J., Homan, J., et al. 2006, *ApJ*, 646, 394
- Muno, M. P., Baganoff, F. K., & Arabadjis, J. S. 2003, *ApJ*, 598, 474
- Muno, M. P., Pfahl, E., Baganoff, F. K., et al. 2005, *ApJL*, 622, L113
- Papitto, A., Ferrigno, C., Bozzo, E., et al. 2013, *Nature*, 501, 517
- Plotkin, R. M., Gallo, E., & Jonker, P. G. 2013, *ApJ*, 773, 59
- Pooley, D., Homan, J., Heinke, C. O., et al. 2011, *The Astronomer's Telegram*, 3627, 1
- Porquet, D., Grosso, N., Burwitz, V., et al. 2005, *A&A*, 430, L9
- Raichur, H., & Paul, B. 2008, *ApJ*, 685, 1109
- Read, A. M., Saxton, R. D., & Esquej, P. 2010a, *The Astronomer's Telegram*, 2607, 1
- Read, A. M., Saxton, R. D., Esquej, P., & Evans, P. A. 2010b, *The Astronomer's Telegram*, 2627, 1
- Reis, R. C., Miller, J. M., & Fabian, A. C. 2009, *MNRAS*, 395, L52
- Reis, R. C., Fabian, A. C., & Miller, J. M. 2010, *MNRAS*, 402, 836
- Remillard, R. A., & McClintock, J. E. 2006, *ARAA*, 44, 49
- Reynolds, M. T., Reis, R. C., Miller, J. M., Cackett, E. M., & Degenaar, N. 2014, *MNRAS*, 441, 3656
- Rutledge, R. E., Bildsten, L., Brown, E. F., Pavlov, G. G., & Zavlin, V. E. 1999, *ApJ*, 514, 945
- Rutledge, R. E., Bildsten, L., Brown, E. F., Pavlov, G. G., & Zavlin, V. E. 2001a, *ApJ*, 551, 921
- Rutledge, R. E., Bildsten, L., Brown, E. F., Pavlov, G. G., & Zavlin, V. E. 2001b, *ApJ*, 559, 1054
- Rutledge, R. E., Bildsten, L., Brown, E. F., Pavlov, G. G., & Zavlin, V. E. 2002a, *ApJ*, 577, 346
- Rutledge, R. E., Bildsten, L., Brown, E. F., et al. 2002b, *ApJ*, 580, 413
- Sakano, M., Warwick, R. S., Decourchelle, A., & Wang, Q. D. 2005, *MNRAS*, 357, 1211
- Shahbaz, T., Russell, D. M., Zurita, C., et al. 2013, *MNRAS*, 434, 2696
- Shinoda, K., Kii, T., Mitsuda, K., et al. 1990, *PASJ*, 42, L27
- Sidoli, L., Paizis, A., Mereghetti, S., Götz, D., & Del Santo, M. 2011, *MNRAS*, 415, 2373
- Tomsick, J. A., Gelino, D. M., Halpern, J. P., & Kaaret, P. 2004, *ApJ*, 610, 933
- Wijnands, R., & van der Klis, M. 1999, *ApJ*, 514, 939
- Wijnands, R., Miller, J. M., & Wang, Q. D. 2002, *ApJ*, 579, 422
- Wijnands, R., Heinke, C. O., Pooley, D., et al. 2005, *ApJ*, 618, 883
- Wijnands, R., in't Zand, J. J. M., Rupen, M., et al. 2006, *A&A*, 449, 1117
- Wijnands, R., Rol, E., Cackett, E., Starling, R. L. C., & Remillard, R. A. 2009, *MNRAS*, 393, 126
- Wijnands, R., Yang, Y. J., Degenaar, N., et al. 2011, *The Astronomer's Telegram*, 3595, 1
- Wijnands, R., & Degenaar, N. 2013, *MNRAS*, 434, 1599
- Yang, Q.-X., Xie, F.-G., Yuan, F., et al. 2015, *MNRAS*, 447, 1692
- Zampieri, L., Turolla, R., Zane, S., & Treves, A. 1995, *ApJ*, 439, 849

Table 1. Neutron-star X-ray transients which have low N_{H}

Source	References	Distance (kpc)	N_{H}^h (10^{22} cm $^{-2}$)	Γ	L_{X} (10^{35} erg s $^{-1}$)
AX J1754.2–2754	Armas Padilla et al. (2013b)	9.2	2.93±0.06	2.51±0.03	2.74±0.08
	Degenaar et al. (2012a) ^a		2.1±0.3	2.8±0.2	2.1±0.2
1RXS J171824.2–402934	Armas Padilla et al. (2013b)	9.0	1.78±0.04	2.33±0.04	0.78±0.01
	in 't Zand et al. (2009)		1.3	2.44±0.1	0.63±0.03
	Campana (2009) ^{b,c}		1.2±0.1	2.37±0.11	0.54±0.03
				2.3±0.3	0.88
				1.9±0.1	3.6
				2.1±0.1	2.1
				2.4±0.1	0.97
				2.4±0.2	0.56
1RXH J173523.7–354013	Armas Padilla et al. (2013b)	9.5	1.43±0.07	2.45±0.07	0.56±0.03
XTE J1709–267	Degenaar et al. (2013)	8.5	0.34±0.03	2.0±0.1	29±2
				2.4±0.1	15±2
				2.6±0.3	0.7±0.1
			0.49±0.01	2.90±0.04	0.201±0.001 ^e
IGR J17062–6143	Degenaar et al. (2012c) ^c	5.0	0.20±0.01	2.1±0.1	6
1RXS J170854.4–321857	in 't Zand et al. (2005)	13.0	0.40±0.01	1.9±0.2	15±1
	Campana (2009) ^c		0.43±0.02	1.98±0.05	33
				2.4±0.1	3.6
SAX J1753.5–2349	Campana (2009) ^c	8.8	1.9 ^{+0.5} _{−0.6}	2.0±0.4	7.7
Swift J174805.3–24463 ^f	Bahramian et al. (2014) ^g	5.9	1.74	2.5±0.4	1.0 ^{+0.3} _{−0.2}
				2.3±0.3	1.5±0.2
				1.9±0.4	3.7±0.5
				1.4±0.1	27.3±1.3
				2.07±0.07	21.3±0.8
				1.7±0.1	12.2±0.7
				1.8±0.1	10.8±0.7
				1.9±0.2	11.0±1.2
				1.8±0.1	9.1±0.5
				1.9±0.2	8.9±0.7
				2.0±0.1	6.2±0.5
				1.8±0.3	4.6±0.5
				2.0±0.2	1.9±0.2
Aql X-1	Gandhi et al. (2014)	5.0	0.95±0.2	2.6±0.3	0.60±0.15
IGR J17494–3030 ^d	Armas Padilla et al. (2013c)	8.0	1.87	1.8±0.2	10.7±0.08
				1.9±0.1	13.4±0.08
				1.8±0.3	8.7±0.08
				2.0±0.3	2.6±0.08
XTE J1719–291 ^d	Armas Padilla et al. (2011)	8.0	0.53	2.02±0.08	13.3±0.8
				2.74±0.05	0.475±0.007
				2.83±0.25	0.36 ^{+0.03} _{−0.02}
				2.6±0.4	0.30 ^{+0.06} _{−0.03}
				2.32±0.11	2.8±0.2
				2.15±0.09	4.4±0.3
				2.7±0.4	0.38 ^{+0.07} _{−0.03}

^a 0.3–10 keV fluxes converted to 0.5–10 keV fluxes using WebPIMMS

^b Luminosities converted to 9 kpc

^c No errors on luminosities (see section 3.4)

^d NS nature not yet confirmed

^e Luminosity calculated from a power-law plus a neutron-star atmosphere model fit to the same spectrum

^f Also known as Terzan 5 X-3; the third bright X-ray transient in the globular cluster Terzan 5

^g Data taken from their Table 9; excluding the data with X-ray luminosities $> 5 \times 10^{36}$ erg s $^{-1}$ and with errors on the photon index > 0.5
^h The column density as obtained in the quoted papers. If no errors are given, the column density was fixed to the value quoted (i.e., for 1RXS J171824.2–402934 the N_{H} used was obtained by in 't Zand et al. (2005) using a higher quality Chandra observation of the source; for Swift J174805.3–24463 the N_{H} used was obtained from quiescent spectra also reported by Bahramian et al. (2014); for IGR J17494–3030 and XTE J1719–291 the reported N_{H} was determined from high quality XMM-Newton data reported in Armas Padilla et al. (2013c) and Armas Padilla et al. (2011), respectively).

Table 2. Black-hole X-ray transients

Source	References	Distance (kpc)	N_{H}^f (10^{22} cm^{-2})	Γ	L_{X} ($10^{35} \text{ erg s}^{-1}$)
Swift J1357.2–0933 ^{a,b}	Armas Padilla et al. (2013a)	1.5	0.012	1.53±0.02	1.13±0.02
				1.58±0.02	1.01±0.01
				1.56±0.01	0.941±0.007
				1.55±0.02	0.708±0.008
				1.57 ^{+0.05} _{-0.06}	0.56±0.02
				1.59±0.02	0.445±0.005
				1.58±0.02	0.346±0.004
				1.61±0.03	0.203±0.004
				1.65±0.05	0.110±0.003
				1.78±0.06	0.059±0.002
				1.9±0.2	0.012±0.001
Plotkin black-hole sample ^{c,d}	Plotkin et al. (2013)	–	–	2.05 ^{+0.21} _{-0.17}	$(4.1 \pm 2.5) \times 10^{-5}$
				2.15 ^{+0.19} _{-0.18}	$(3.3 \pm 1.8) \times 10^{-4}$
				1.98 ^{+0.10} _{-0.11}	$(4.4 \pm 1.7) \times 10^{-3}$
				2.02±0.06	$(3.7 \pm 2.1) \times 10^{-2}$
				1.67±0.08	0.43 ± 0.09
Swift J1753.5–0217	Reis et al. (2010) ^e	8.5	0.175±0.001	1.666±0.003	35.44±0.09
GRO J1655–40	Reis et al. (2010) ^e	3.2	0.525±0.003	1.660±0.005	11.6±0.2
XTE J1118+480	Reis et al. (2010) ^e	1.72	0.0080±0.0001	1.877±0.005	4.60±0.04
MAXI J1659–152	Jonker et al. (2012)	6	0.27±0.01	1.48±0.03	0.82±0.09
H 1743–322	Jonker et al. (2010)	8.5	2.3	1.74±0.05	25.3±0.5
				1.59±0.08	9.2±0.3
				1.70±0.08	3.29±0.09
				1.6±0.1	1.82±0.09
				1.9±0.2	0.66±0.05

^a Strong BH candidate

^b Using the averaged data; data points not tabulated in Armas Padilla et al. (2013a)

^c Using the averaged data as calculated from their Table 3 and 5

^d The luminosity errors correspond to the standard deviation on the luminosity points use to calculate the average

^e 0.5–10 keV fluxes obtained using a more complex model.

^f The column density as obtained in the quoted papers. If no errors are given, the column density was fixed to the value quoted (i.e., for Swift J1357.2–0933 the N_{H} used was obtained by Armas Padilla et al. (2014a) using a high quality XMM-Newton observation of the source; for H 1743–322 the N_{H} used was obtained from high quality outburst spectra reported by Miller et al. (2006).)

Table 3. Neutron-star X-ray transients which are also AMXPs

Source	References	Distance (kpc)	N_{H}^e (10^{22} cm^{-2})	Γ	L_{X} ($10^{35} \text{ erg s}^{-1}$)
NGC 6440 X-2	Heinke et al. (2010) ^a	8.5	0.59	2.4±0.5	0.33±0.08
				2.3±0.4	0.31±0.06
				1.8±0.2	5.9±0.6
				1.9±0.3	1.0 ^{+0.2} _{-0.1}
				1.7±0.1	5.5±0.3
				2.3 ^{+0.3} _{-0.4}	0.9±0.1
IGR J00291+5934	Lewis et al. (2010) ^b	3	0.69±0.06	1.8±0.1	15.5±0.6
			0.6±0.1	1.7±0.1	5.2±0.2
			0.5±0.1	1.6±0.1	2.1±0.2
IGR J18245–2452	Linares et al. (2014) ^c	5.5	0.32±0.02	1.34±0.04	18.7±0.9
			0.44±0.02	1.37±0.02	36.9±1.1
			0.33±0.02	1.31±0.04	40.2±2.0
			0.38±0.02	1.26±0.03	48.1±2.2
			0.38±0.04	1.23±0.05	28.7±2.1
			0.43±0.04	1.47±0.05	15.5±1.1
			0.30±0.08	1.50±0.14	1.9±0.3
			0.51±0.06	1.30±0.08	7.6±0.8
			0.46±0.02	1.50±0.03	32.8±1.1
			0.42±0.04	1.53±0.07	6.9±0.6
			0.37±0.04	1.41±0.07	12.7±1.1
			0.51±0.07	1.66±0.10	7.8±0.9
			0.41±0.02	1.46±0.03	17.5±0.8
			0.39±0.02	1.37±0.02	27.0±0.9
0.34±0.02	1.51±0.03	12.2±0.5			
0.44±0.04	1.56±0.05	5.4±0.4			
0.4±0.1 ^d	2.4±0.2	0.4±0.2			

^a Data points taken from their Table 1 using the same criteria as for the non-pulsating sources.

^b Data points taken from their Table 6; 2–10 keV fluxes converted to 0.5–10 keV fluxes using WebPIMMS.

^c Data points not tabulated by Linares et al. (2014).

^d We used the average data for the observations taken between April 15–17, 2013.

^e The column density as obtained in the quoted papers. If no errors are given, the column density was fixed to the value quoted (i.e., for NGC 6440 X-2 the N_{H} used was fixed to the cluster value.)

Table 4. Neutron-star X-ray transients which have high N_{H}

Source	References	Distance (kpc)	N_{H}^c (10^{22} cm^{-2})	Γ	L_{X} ($10^{35} \text{ erg s}^{-1}$)
GRS 1741–2853	Degenaar et al. (2012b) ^a	7.2	11.4 ± 1.1	2.0 ± 0.3	2.8 ± 0.3
				1.5 ± 0.2	3.3 ± 0.2
				1.6 ± 0.4	0.76 ± 0.04
AX J1745.6–2901	Degenaar et al. (2012b) ^a	8	21.8 ± 0.3	1.9 ± 0.1	8.0 ± 0.3
				1.6 ± 0.1	39.8 ± 0.9
				1.8 ± 0.1	32.4 ± 0.9
				1.6 ± 0.1	42.2 ± 0.9
				1.8 ± 0.1	39.0 ± 1.0
SAX J1747.0–2853	Degenaar et al. (2012b) ^a	6.7	9.5 ± 0.2	1.6 ± 0.1	17.3 ± 0.5
				2.0 ± 0.1	39.1 ± 0.5
				2.6 ± 0.1	18.6 ± 0.2
KS 1741–293	Degenaar et al. (2012b) ^a	8	16.6 ± 1.8	1.8 ± 0.3	2.2 ± 0.2
XMMU J1747161–281048	Del Santo et al. (2007) ^a	8.4	8.9 ± 0.5	2.1 ± 0.1	1.15 ± 0.07
	Degenaar et al. (2011) ^{a,b}	8.4	8.6 ± 2.3	2.2 ± 0.5	1.2

^a 2–10 keV fluxes converted to 0.5–10 keV fluxes using WebPIMMS

^b No errors on the flux (see section 3.4)

^c The column density as obtained in the quoted papers

APPENDIX A: THE TRANSIENT IN NGC 6388

The transient IGR J17361–4441 was discovered using INTEGRAL in August 2011 (Gibaud et al. 2011). The source position is consistent with that of the globular cluster NGC 6388 (Ferrigno et al. 2011). Its location in a globular cluster suggests that if the source is an X-ray binary, the accretor is accreting matter from a low-mass companion star. *Swift*/XRT follow-up observations showed a very hard source with a photon index ~ 1 (Ferrigno et al. 2011; Wijnands et al. 2011; Bozzo et al. 2011). Such a hard index is atypical for neutron-star or black-hole X-ray transients. It has been suggested it could be a X-ray transient harbouring a strong magnetic field neutron star (Wijnands et al. 2011) since such systems have typically similarly hard spectra (e.g., Becker et al. 1977; Giles et al. 1996). Alternatively it could be an intermediate mass black hole (Wijnands et al. 2011) but the source position is not exactly in the center of the cluster and therefore this scenario is unlikely (Pooley et al. 2011). Recently, it was suggested (Del Santo et al. 2014) that the transient could be a tidal disruption event, in which a planetary sized body was disrupted by an heavy white dwarf (with a mass close to the Chandrasekhar limit).

At the time when the transient was discovered with INTEGRAL, we requested a DDT observation on *XMM-Newton* to study the X-ray spectrum of this source in detail. This request was approved and the observation was performed on 23 September 2011 for an on-source exposure time of ~ 43 ksec. The spectral results of this observation will be reported elsewhere (Armas Padilla et al. 2015 in preparation) but also during the *XMM-Newton* observation the source displayed a very hard spectrum (consistent with the Swift/XRT results). During the *XMM-Newton* observation we used the EPIC-pn camera in timing mode to avoid pile-up and to be able to search for X-ray pulsations and aperiodic rapid X-ray variability. We find no evidence for coherent pulsations, however, we do detect strong aperiodic variability (including a quasi-periodic oscillation or QPO).

We applied the standard reduction on the pn data. Since the pn was used in timing mode, one of the spatial dimensions was collapsed and the normal practice of extracting the source data using a circle around the source position cannot be applied. Therefore, as source and background events we extracted the data using the RAWX columns [36:39] and [9:12], respectively. Both the source and the background were extracted in the energy range 0.5–10 keV. We rebinned the pn data to a time-resolution of 1 msec and then used a fast fourier transform to create ~ 4300 s long power density spectra of the source. All data were added to create one spectrum. The spectrum was renormalized using the background count rate obtained from the background data. The Poisson level was estimated from frequencies above 15 Hz and then subtracted from the power spectrum. The resulting power spectrum is shown in Figure A1. Clearly strong band limited noise is seen together with a narrow QPO at around 0.01 Hz. We fit the QPO with a Lorentzian and the band-limited noise with a broken power-law model. The errors were estimated using $\Delta\chi^2 = 1.0$. For the QPO we obtained a frequency of 0.1026 ± 0.0009 Hz, a fractional rms amplitude of $17.2\% \pm 0.7\%$ (0.5–10 keV), and a FWHM of 0.022 ± 0.002 Hz. For the band-limited noise we obtained a break frequency of

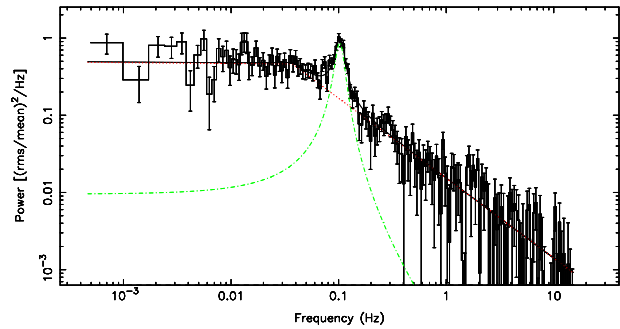


Figure A1. The power density spectrum obtained using the *XMM-Newton* pn timing data of the transient in NGC 6388.

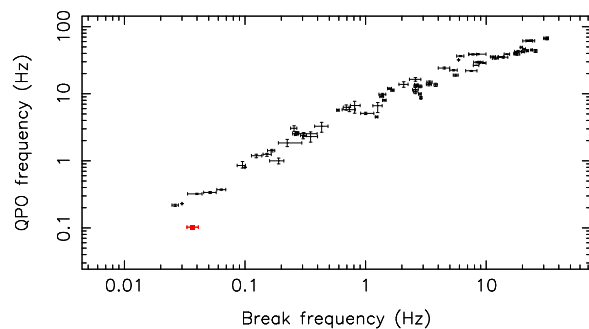


Figure A2. The break frequency versus the QPO frequency. The black points are from Wijnands & van der Klis (1999) and the red point is for the transient in NGC 6388. (A colour version of this figure is available in the online version of this paper.)

0.037 ± 0.004 Hz, an index of 0.01 ± 0.06 below the break and 1.03 ± 0.04 above the break and a fractional rms amplitude (integrated over 0.001 to 100 Hz; 0.5–10 keV) of $37\% \pm 2\%$.

The power spectrum of the source is a typical one seen often from low-mass X-ray binaries (both neutron-star as well as black-hole systems) accreting at relatively low luminosities. The indices of the band-limited noise are very typical: ~ 0 before the break frequency and ~ 1 above. The strength of the noise is also very typical. The break frequency and the QPO frequency are very low, but also what has been seen before in X-ray binaries. To highlight this, we plotted the QPO frequency versus the break frequency in Figure A2 and compared it with the data points reported by Wijnands & van der Klis (1999). Although the QPO frequency seems a bit low compared to the other sources, the source is still consistent with the Wijnands & van der Klis relation when taking into account the scatter (see the discussion in Wijnands & van der Klis 1999).

In accreting high-magnetic field neutron-star systems, often low-frequency QPOs are also observed (e.g., Belloni & Hasinger 1990; Shinoda et al. 1990; Chakrabarty 1998; Raichur & Paul 2008; James et al. 2010, 2011). Although also band-limited noise is often observed, it does not have the typical broken power law shape we observe for IGR J17361–4441. Therefore, we think it is unlikely that the source is a high-magnetic field neutron-star system. The aperiodic variability of the source shows that most likely the source is an accreting neutron star or black hole in a low-

mass X-ray binary. The unusually hard spectrum still needs to be explained.

Bozzo et al. (2014) also reported the discovery of the QPO in IGR J173611–4441. They argue that the characteristics of the QPO are compatible with the tidal disruption event scenario proposed by Del Santo et al. (2014). Bozzo et al. (2014) rejected a neutron-star X-ray binary possibility based on the fact that such systems hardly show QPOs at such low frequencies. However, we disagree with this statement since such low frequency QPOs have indeed been reported for neutron-star systems (see, e.g., Linares et al. 2007). Therefore, although we cannot exclude the tidal disruption event hypothesis, we do consider it more likely that this system is an unusual accreting neutron-star or black-hole binary.